THE JOURNAL OF PHYSICAL CHEMISTRY Letters

LETTER

pubs.acs.org/JPCL

Graphenes Converted from Polymers

Sun-Jung Byun,[†] Hyunseob Lim,[‡] Ga-Young Shin,[†] Tae-Hee Han,[†] Sang Ho Oh,[†] Jong-Hyun Ahn,[ξ] Hee Cheul Choi,[‡] and Tae-Woo Lee*[,†]

[†]Department of Materials Science and Engineering, Pohang University of Science and Technology (POSTECH), Pohang, Gyungbuk 790-784, Republic of Korea

[‡]Department of Chemistry, Pohang University of Science and Technology, Pohang, Gyungbuk 790-784, Republic of Korea

[ξ]School of Advanced Materials Science and Engineering, Sungkyunkwan University, Suwon 440-746, Republic of Korea

Supporting Information

ABSTRACT: Because the direct formation of large, patterned graphene layers on active electronic devices without any physical transfer process is an ultimate important research goal for practical applications, we first developed a cost-effective, scalable, and sustainable process to form graphene films from solution-processed common polymers directly on a SiO_2/Si substrate. We obtained few-layer graphene by heating the thin polymer films covered with a metal capping layer in a high-temperature furnace under low vacuum in an Ar/H_2 atmosphere. We find that the metal capping layer appears to have two functions: prevention of vaporization of dissociated molecules and catalysis of graphene formation. We suggest that polymer-derived graphene growth directly on inert substrates in active electronic devices will have great advantages because of its simple, inexpensive, and safer process.

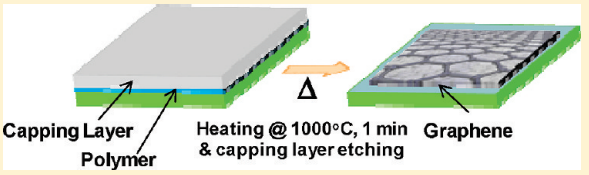

SECTION: Macromolecules, Soft Matter

Graphene has been attracting great interest because of its outstanding electronic, mechanical, and chemical properties since it was first produced by mechanical exfoliation in 2004.[1−5] Several methods of fabricating large graphene sheets are known,[1−24] but realization of these applications requires a method of synthesizing large uniform graphene sheets that can be scaled up to industrial production levels. Recently, chemical vapor deposition (CVD) of CH_4 or C_2H_2 gases and solid carbon sources on catalytic metal (Ni or Cu) substrates has been demonstrated as an attractive method to synthesize large-area graphene for practical applications.[17−25] However, additional physical transfer processes of grown graphene films to a receiver substrate are essentially required to be useful in electronic devices.[17−25] During these processes, special care should be taken to avoid severe degradation of the graphene quality and properties. Therefore, a new process to grow and pattern graphene films directly on the electronic devices will have great advantages for scalable practical applications.

In this work, we introduce an unprecedented method that generates graphene sheets from common inexpensive polymers on inert substrates (e.g., SiO_2). Because polymers can be easily deposited on any substrate and can be patterned using simple digital lithography (inkjet printing)[26] or soft lithography,[27] this method of converting polymers to patterned graphene on an inert substrate may accelerate the adoption of graphene films in practical electronics. Moreover, it may have other great advantages because common polymers such as polystyrene (PS), polyacrylonitrile (PAN), and polymethylmetacrylate (PMMA) are inexpensive and safe to handle, unlike explosive gaseous raw carbon sources used in a CVD process.

As the first step toward our ultimate goal of direct formation of large, patterned graphene layers on active electronic devices, we developed a scalable and sustainable process to form graphene films from those common polymers on a SiO_2/Si substrate. We obtained few-layer graphene by capping the films with a metallic layer, then heating them in a high temperature furnace under low vacuum in an Ar/H_2 atmosphere.

In the basic process (Figure 1a), PS (Sigma-Aldrich, weight-average molecular weight M_w = 130 000 g/mol), PAN (Sigma-Aldrich, M_w = 150 000 g/mol), and PMMA (synthesized in the laboratory, number-average molecular weight M_n = 130 000 g/mol) (Figure 1b) were dissolved separately in chloroform (Anhydrous, Sigma-Aldrich) and dimethylformamide (DMF, Extras Pure grade, DAE JUNG chemicals) solvents. SiO_2 (300 nm)/Si substrates (2 × 2 cm^2) were UV/ozone-treated for 30 min before spin coating to make the substrates hydrophilic. The PS, PMMA, and PAN solutions were spin coated on the SiO_2/Si substrates to fabricate polymer thin films with 10 nm thickness.

Such polymers have distinct thermal decomposition temperatures T_d (PS: ∼300 °C, PAN: ∼235 °C, PMMA: ∼310 °C).[28] When the polymers are heated above T_d, their chemical bonds tend to dissociate. An important requirement for graphene precursors is that the molecular backbone of polymers should be composed entirely of carbon atoms, which would become the main source of sp^2 hybridized carbon bonds in graphene sheets.

Received: January 1, 2011
Accepted: February 9, 2011
Published: February 18, 2011

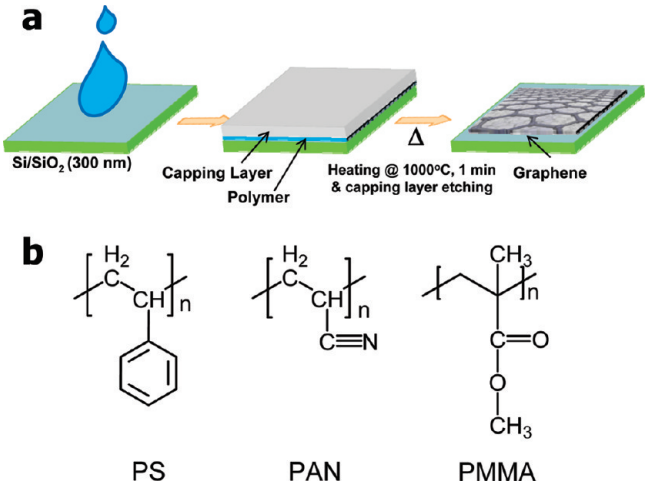

Figure 1. (a) Graphene growth process and (b) chemical structure of polymers used as graphene precursors.

Precursors composed of aliphatic C−C single bonds are preferable because they have lower bond dissociation energies (284−368 kJ/mol) than C═C (615 kJ/mol), C≡C (812 kJ/mol), and aromatic/heterocyclic C−C (410 kJ/mol).[28] We chose the vinyl polymers PS, PAN, and PMMA as graphene precursors because we thought that their planar zigzag configuration may facilitate cyclization of C−C bonds.

In initial trials, we tried to use a process to convert 10 nm thick polymer thin films on 300 nm SiO_2/Si substrates to graphene films in a furnace with Ar (50 sccm) and H_2 (10 sccm) gas flow under vacuum (4.0 Torr) at 1000 °C for 1 min. The Raman spectra and mapping images were obtained using a WITEC Raman system with excitation of 532 nm. Raman spectroscopy (Figure 2a) did not reveal any peaks related to graphene or polymers. Even if we have tried the thermal conversion of polymers to graphene on catalytic Ni (300 nm)/SiO_2(300 nm)/Si substrates many times, we have not observed any Raman peaks related to the graphenes from the samples (Figure 2b), which is contradictory to the very recent report regarding the growth of graphene from organic materials on the Ni catalyst.[25] Our Raman data indicate that most compounds formed by dissociation of the polymers were removed from the substrates during pyrolysis because of vaporization in the furnace and then evacuated without readsorption on the substrate.

To prevent this vaporization, we formed a metal capping layer of Ni or Cu atop the PAN/SiO_2/Si substrates. We pyrolized PAN films at 800 or 1000 °C in the furnace under Ar (50 sccm) and H_2 (10 sccm) gas; then, we used Raman spectroscopy to observe the carbonization of the polymers.[29,30] Pyrolysis at 800 °C did not result in the formation of graphenes: broad peaks occurred around 1350 (D band) and 1580 cm^{-1} (G band) but not at ~2700 cm^{-1} (2D bands) (Figure 2b). These results indicate that the pyrolysis converted the polymers to amorphous carbons.[30] Pyrolysis at 1000 °C resulted in the formation of graphenes: Two distinct peaks occurred at 1586 (G band) and 2705 cm^{-1} (2D band) (Figure 3a). This result is consistent with the Raman spectra of graphenes grown by CVD.[17−24] Comparison of our Raman spectrum with one for CVD-grown graphenes[17] suggests that our graphene consists of approximately three layers (Figure 3a); this result is consistent with our high-resolution transmission electron microscopy (HRTEM) results, which suggest three to five layers (Figure 3c,d). The 2D band of our graphene has full width at half-

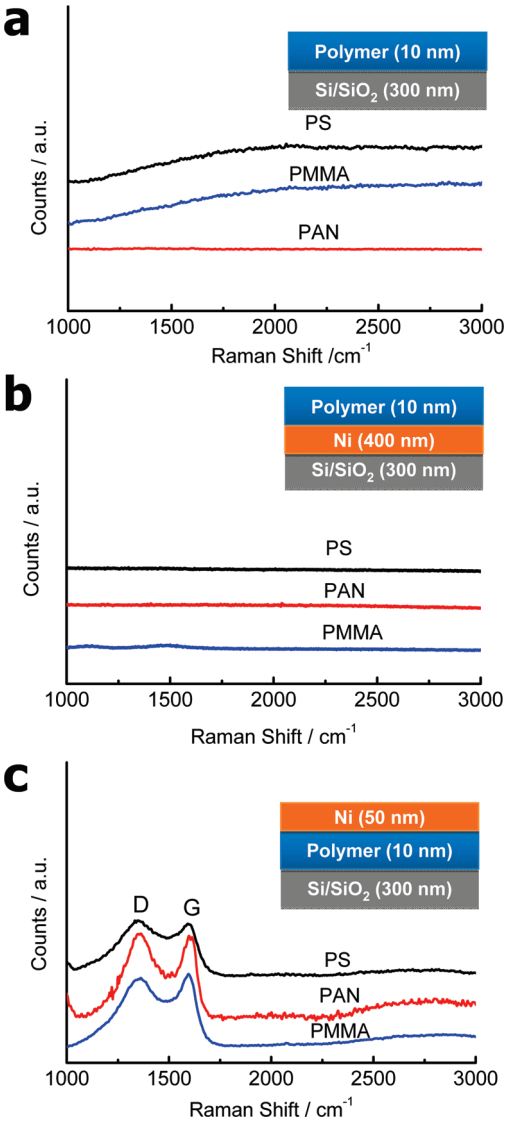

Figure 2. Raman spectra after pyrolysis. (a) After pyrolysis of polymer films without a capping layer at 1000 °C. (b) After pyrolysis of polymer films on a 400 nm thick Ni catalyst layer at 1000 °C. (c) After pyrolysis of polymer films with a 50 nm thick Ni capping layer at 800 °C.

maximum (fwhm) of ~89 cm^{-1}, which is also similar to the fwhm of CVD-grown three-layer graphene (~82 cm^{-1}). We observed a relatively small peak at 1352 cm^{-1} (D band). The D-to-G band peak intensity ratio (I_D/I_G) was 0.168; therefore, in this current research stage of this new method, further optimization is required to reduce further the intensity of the D band.

In Raman spectra maps (Figure 3b) of the D, G, and 2D bands, the bright spots of G and 2D bands were distributed homogeneously on the surface, because of agglomeration of the Ni capping layer. The grain size of graphene in the bright spots was estimated to be 1.249 ± 0.215 μm. However, according to further detailed Raman analysis, we demonstrated that graphene films synthesized from PAN covers most of substrate above 95.33% (or only 4.67% regions showed noise-level Raman signal) (Supporting Information, Figure S1).

We observed similar Raman spectra after removing a 50 nm thick Ni capping layer (Supporting Information, Figure S2); this means that the graphene films were also formed underneath the Ni capping

dx.doi.org/10.1021/jz200001g |J. Phys. Chem. Lett. 2011, 2, 493–497

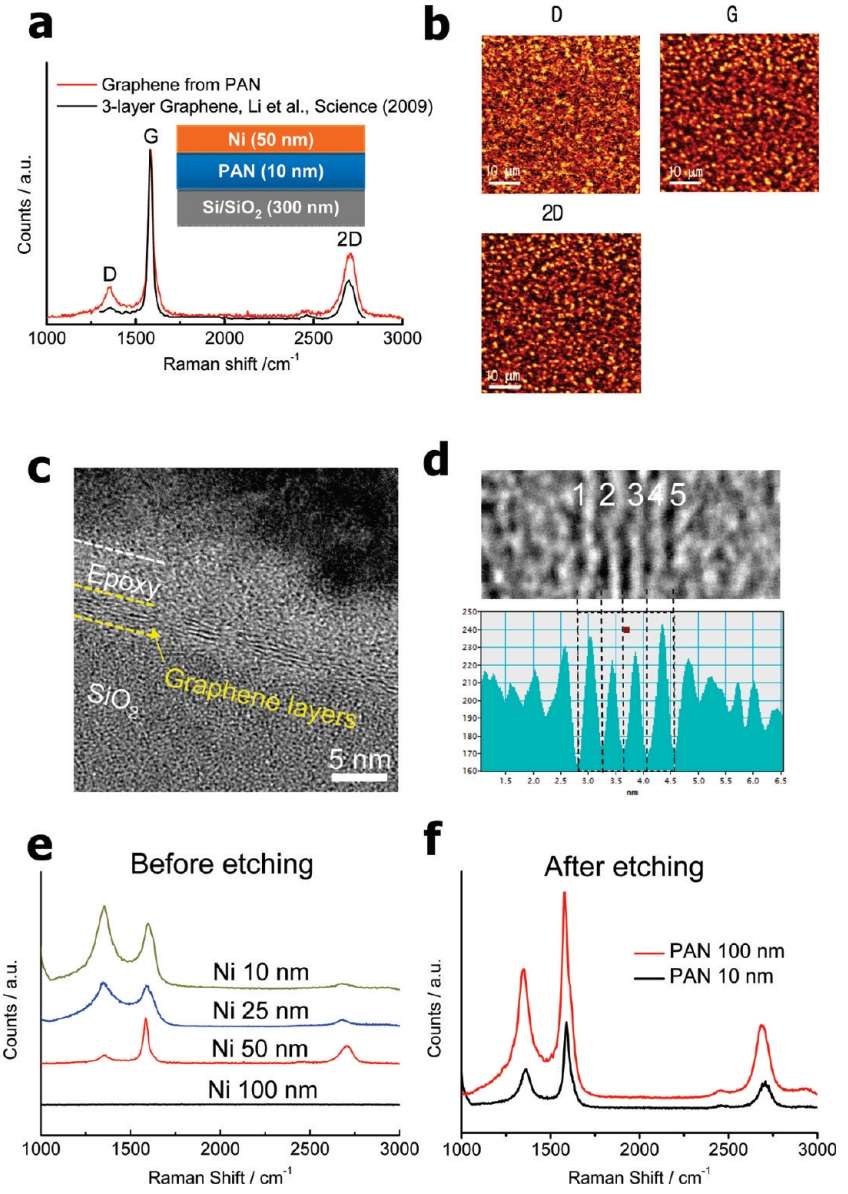

Figure 3. Properties of PAN-derived graphenes: (a) Raman spectra after pyrolysis of PAN polymer films with a 50 nm thick Ni capping layer at 1000 °C before removing the capping layer. (b) Raman spectra D, G, and 2D bands maps (50 μm × 50 μm) after pyrolysis of polymer films with a 50 nm thick Ni capping layer at 1000 °C. (c) Cross-sectional HRTEM image of the graphenes formed on SiO_2/Si substrate outside agglomerated Ni islands. (d) Magnified HRTEM image and the intensity profile across the graphenes. (e) Raman spectra of PAN-derived graphene depending on the thickness of Ni capping layer before removing the capping layer. (f) Raman spectra of PAN-derived graphene depending on the polymer layer thickness after removing the capping layer.

layer and on the SiO_2 substrate outside agglomerated Ni islands, as confirmed by HRTEM results (Figure 3c). However, the graphene films on top of Ni islands were removed during Ni etching process. Some parts of the graphene films underneath the Ni islands can also be removed together during the etching process. Finally, we estimated that the percentage of noise-level Raman signal was estimated to be 17.15%, which indicates that the area covered with graphenes was reduced after Ni etching (Supporting Information, Figure S3).

When thinner capping layers (10 and 25 nm) were employed, Raman spectra revealed strong D bands and a very weak 2D band because of very small coverage after agglomeration (Figure 3e). This indicates that the metal capping layer also functions as a catalyst for graphene formation similarly to the recent conversion processes of amorphous SiC and carbon films to graphene.[31,32] Indeed, the type of metal capping layer is important because the graphene growth mechanism using Ni would not be the same as that when using Cu.[33] For example, graphene is chemisorbed relatively strongly on Ni but weakly on Cu.[34] We verified this conjecture by preparing with Ni or Cu capping layers. The Ni capping layer helped to form graphenes better than did Cu under the same experimental conditions (Supporting Information, Figures S4 and S5) because carbon atoms are much more soluble in Ni[35] than in Cu.[36]

The thickness of the metal capping layer is also important because if it is too thin (<50 nm), then the metal easily agglomerated and partially departed from the substrate at high temperature. When we used a thinner metal capping layer (10 and 25 nm), the conversion from the polymer to graphene was not successful because of the strong agglomeration of the metal capping layers and very small

dx.doi.org/10.1021/jz200001g |J. Phys. Chem. Lett. 2011, 2, 493–497

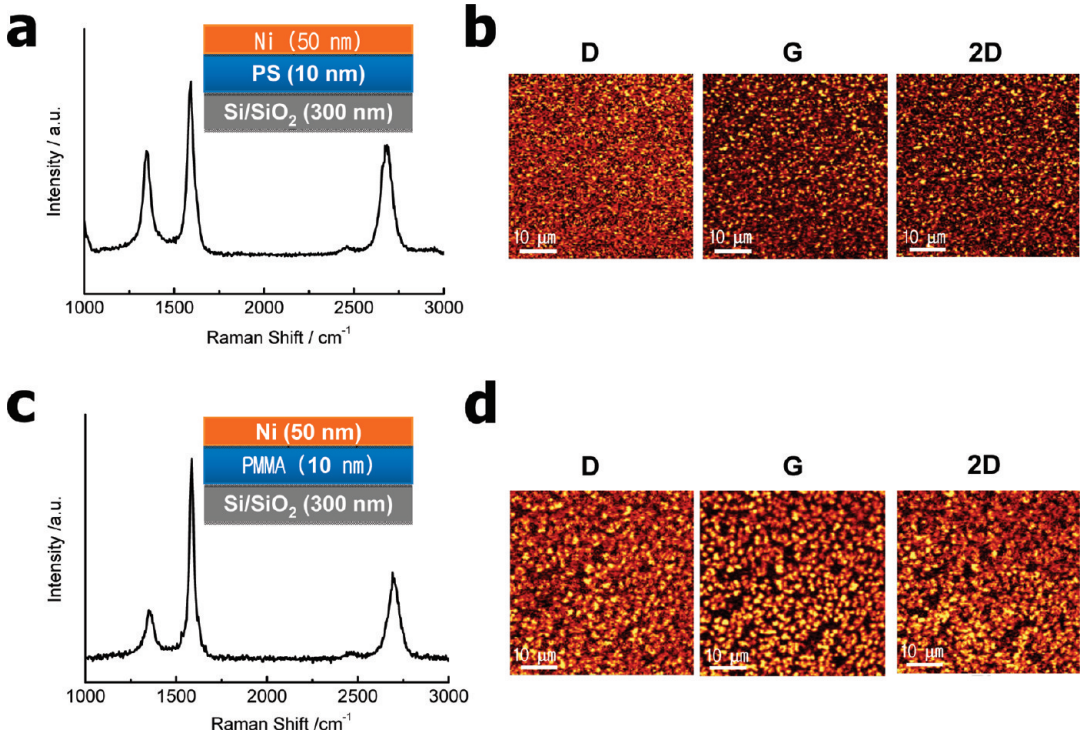

Figure 4. Raman spectra of PS and PMMA-derived graphene: (a) Raman spectra after pyrolysis of PS polymer films with a 50 nm thick Ni capping layer at 1000 °C. (b) Raman spectra D, G, and 2D band maps (50 μm × 50 μm) after pyrolysis of PS polymer films with a 50 nm thick Ni capping layer at 1000 °C. (c) Raman spectra after pyrolysis of PMMA polymer films with a 50 nm thick Ni capping layer at 1000 °C. (d) Raman spectra D, G, and 2D band maps after pyrolysis of PMMA polymer films with a 50 nm thick Ni capping layer at 1000 °C.

coverage of the polymer film surface (Figure 3e). Therefore, the carbon films obtained from conversion of PAN films were more amorphous under 10 or 25 nm thick Ni capping layers than under 50 nm layers. These results suggest that graphene forms under the Ni capping layer as a result of carbon diffusion into the metal and subsequent precipitation as a graphene layer on the metal surface upon cooling.[33] In contrast, we did not observe distinct Raman peaks from the top surface of the Ni when we used a 100 nm thick Ni capping layer (Figure 3e). This implies that the dissociated carbon atoms or aliphatic molecules generated by pyrolysis cannot diffuse completely into the 100 nm thick Ni layer at 1000 °C during such a short time of 1 min, and thus precipitation of carbon at the top surface after cooling could not take place. We also observed the dependence of the polymer film thickness (Figure 3f). As we increased the film thickness from 10 to 100 nm, the D band tended to be stronger, implying the formation of graphenes with more defects. The polymer close to the Ni capping layer in the thicker polymer film is likely to be converted to higher quality graphene, whereas the polymer close to the SiO_2/Si substrate is likely to be converted to lower quality graphene including partial amorphous carbon regions. Therefore, thinner films turned out to be better to improve the graphene quality.

Additional experiments are required to elucidate the precise mechanism of graphene formation in this system. Technical implementation of this fabrication method for practical electronics faces some challenges such as prevention of metal capping layer agglomeration and control of number of the graphene layers. We believe that the number of graphene layers and the uniformity can be controlled by optimizing the cooling rate as well as pyrolysis conditions and the type of metal capping layer.

We performed the same experiments using PS and PMMA precursors instead of PAN (Figure 4). In the case of PS, we observed strong G and 2D peaks, but the D peak was more pronounced than that when using PAN, which might be attributed to the higher dissociation energy of aromatic carbon pendants. However, graphene yield using PMMA was similar to that obtained using PAN. Therefore, we demonstrate that the graphene formation from common polymers is not limited to specific polymers. PAN unlike PS and PMMA is also known as a precursor of carbon fibers because of efficient graphitization at very high temperatures (2000−3000 °C).[37] The successful few-layer-graphene formation from PS and PMMA as we achieved from PAN indicates that the carbonization mechanism is different from the general graphitization process from pyropolymers to carbon fibers.

In conclusion, we demonstrated a cost-effective, scalable and sustainable process to fabricate graphene films from common vinyl polymer thin films on inert substrates under a metal capping layer. We achieved graphene films of a few layers by brief pyrolysis at 1000 °C for 1 min under a 50 nm thick Ni capping layer. The metal capping layer appears to have two functions: prevention of vaporization of dissociated molecules and catalysis of graphene formation. Our approaches may provide a method of forming large, patterned graphene layers directly on electronic devices without using any transfer process.

■ ASSOCIATED CONTENT

Ⓢ Supporting Information. Analysis of uniformity of graphene films by Raman spectroscopy before Ni etching, Raman spectroscopy data of PAN-derived graphenes after 50 nm Ni etching, analysis of uniformity of graphene films by Raman spectroscopy after Ni etching, Raman spectroscopy data of films

after pyrolysis of Si/SiO2/PAN (10 nm)/Cu (100 nm) before Cu etching, Raman spectroscopy data of films after pyrolysis of Si/SiO_2/PAN (10 nm)/Cu (100 nm) after Cu etching, and experimental procedures. This material is available free of charge via the Internet http://pubs.acs.org.

AUTHOR INFORMATION

Corresponding Author

*Tel: +82-54-279-2151. Fax: +82-54-279-2399. E-mail: twlee@postech.ac.kr.

ACKNOWLEDGMENT

This research was supported by the Basic Research Program through the National Research Foundation of Korea (NRF), funded by the Ministry of Education, Science and Technology (nos. 2010-0028038, 2010-0015245, and 2010-0016002).

REFERENCES

(1) Geim, A. K. Graphene: Status and Prospects. *Science* **2009**, *324*, 1530–1534.

(2) Wei, D.; Liu, Y. Controllable Synthesis of Graphene and Its Applications. *Adv. Mater.* **2010**, *22*, 3225–3241.

(3) Rao, C. N. R.; Sood, A. K.; Subrahmanyam, K. S.; Govindaraj, A. Graphene: The New Two-Dimensional Nanomaterials. *Angew. Chem., Int. Ed.* **2009**, *48*, 7752–7777.

(4) Allen, M. J.; Tung, V. C.; Kaner, R. B. Honeycomb Carbon: A Review of Graphene. *Chem. Rev.* **2010**, *110*, 132–145.

(5) Wang, G.; Kim, Y.; Choe, M.; Kim, T.-W.; Lee, T. A New Approach for Molecular Electronic Junctions with a Multilayer Graphene. *Adv. Mater.* **2011**, *23*, 755–760.

(6) Park, S.; Ruoff, R. S. Chemical Methods for the Production of Graphenes. *Nat. Nanotechnol.* **2009**, *4*, 217–224.

(7) Cai, J.; Ruffieux, P.; Jaafar, R.; Bieri, M.; Braun, T.; Blankenburg, S.; Muoth, M.; Seitsonen, A. P.; Saleh, M.; Feng, X.; Müllen, K.; Fasel, R. Atomically Precise Bottom-up Fabrication of Graphene Nanoribbons. *Nature* **2010**, *466*, 470–473.

(8) Zhang, W.; Cui, J.; Tao, C.-A.; Wu, Y.; Li, Z.; Ma, L.; Wen, Y.; Li, G. A Strategy for Producing Pure Single-Layer Graphene Sheets Based on a Confined Self-Assembly Approach. *Angew. Chem., Int. Ed.* **2009**, *48*, 5864–5868.

(9) Zhu, Y.; Murali, S.; Cai, W.; Li, X.; Suk, J. W.; Potts, J. R.; Ruoff, R. S. Graphene and Graphene Oxide: Synthesis, Properties, and Applications. *Adv. Mater.* **2010**, *22*, 3906–3924.

(10) Zhou, Y.; Loh, K. P. Making Patterns on Graphene. *Adv. Mater.* **2010**, *22*, 3615–3620.

(11) Moon, I. K.; Lee, J.; Ruoff, R. S.; Lee, H. Reduced Graphene Oxide by Chemical Graphitization. *Nature Commun.* **2010**, *1*, 73.

(12) Yu, D.; Dai, L. Self-Assembled Graphene/Carbon Nanotube Hybrid Films for Supercapacitors. *J. Phys. Chem. Lett.* **2010**, *1*, 467–470.

(13) Zhou, X.; Liu, Z. A Scalable, Solution-Phase Processing Route to Graphene Oxide and Graphene Ultralarge Sheets. *Chem. Commun.* **2010**, *46*, 2611.

(14) Zhao, J.; Pei., S.; Ren, W.; Gao, L.; Cheng, H.-M. Efficient Preparation of Large-Area Graphene Oxide Sheets for Transparent Conductive Films. *ACS Nano* **2010**, *4*, 5245–5252.

(15) Su, C.-Y.; Xu, Y.; Zhang, W.; Zhao, J.; Tang, X.; Tsai, C.-H.; Li, L.-J. Electrical and Spectroscopic Characterizations of Ultra-Large Reduced Graphene Oxide Monolayers. *Chem. Mater.* **2009**, *21*, 5674–5680.

(16) Emtsev, K. V.; et al. Towards Wafer-Size Graphene Layers by Atmospheric Pressure Graphitization of Silicon Carbide. *Nat. Mater.* **2009**, *8*, 203–207.

(17) Li, X.; Cai, W.; An, J.; Kim, S.; Nah, J.; Yang, D.; Piner, R.; Velamakanni, A.; Jung, I.; Tutuc, E.; Banerjee, S. K.; Colombo, L.; Ruoff, R. S. Large-Area Synthesis of High-Quality and Uniform Graphene Films on Copper Foils. *Science* **2004**, *324*, 1312–1314.

(18) Kim, K. S.; Zhao, Y.; Jang, H.; Lee, S. Y.; Kim, J. M.; Kim, K. S.; Ahn, J.-H.; Kim, P.; Choi, J.-Y.; Hong, B. H. Large-Scale Pattern Growth of Graphene Films for Stretchable Transparent Electrodes. *Nature* **2009**, *457*, 706–710.

(19) Bae, S.; et al. Roll-to-Roll Production of 30-in. Graphene Films for Transparent Electrodes. *Nat. Nanotechnol.* **2010**, 574–578.

(20) Reina, A.; Jia, X.; Ho, J.; Nezich, D.; Son, H.; Bulovic, V.; Dresselhaus, M. S.; Kong, J. Large Area, Few-Layer Graphene Films on Arbitrary Substrates by Chemical Vapor Deposition. *Nano Lett.* **2009**, *9*, 30–35.

(21) Bhaviripudi, S.; Jia, X.; Dresselhaus, M. S.; Kong, J. Role of Kinetic Factors in Chemical Vapor Deposition Synthesis of Uniform Large Area Graphene Using Copper Catalyst. *Nano Lett.* **2010**, *10*, 4128–4133.

(22) Gao, L.; Ren, W.; Zhao, J.; Ma, L.-P.; Chen, Z.; Cheng, H.-M. Efficient Growth of High-Quality Graphene Films on Cu Foils by Ambient Pressure Chemical Vapor Deposition. *Appl. Phys. Lett.* **2010**, *97*, 183109.

(23) Chae, S. J.; et al. Synthesis of Large-Area Graphene Layers on Poly-Nickel Substrate by CVD: Wrinkle Formation. *Adv. Mater.* **2009**, *21*, 2328–2333.

(24) Zhang, Y.; Gomez, L.; Ishikawa, F. N.; Madaria, A.; Ryu, K.; Wang, C.; Badmaev, A.; Zhou, C. Comparison of Graphene Growth on Single-Crystalline and Polycrystalline Ni by Chemical Vapor Deposition. *J. Phys. Chem. Lett.* **2010**, *1*, 3101–3107.

(25) Sun, Z.; Yan, Z.; Yao, J.; Beitler, E.; Zhu, Y.; Tour, J. M. Growth of Graphene from Solid Carbon Sources. *Nature* **2010**, *468*, 549–552.

(26) Wang, J. Z.; Zheng, Z. H.; Li, H. W.; Huck, W. T. S.; Sirringhaus, H. Dewetting of Conducting Polymer Inkjet Droplets on Patterned Surfaces. *Nat. Mater.* **2004**, *3*, 171–176.

(27) Granlund, T.; Nyberg, T.; Roman, L. S.; Svensson, M.; Inganäs, O. Patterning of Polymer Light-Emitting Diodes with Soft Lithography. *Adv. Mater.* **2000**, *12*, 269–272.

(28) Mark, J. E. *Physical Properties of Polymers Handbook*; Springer: New York, 2007; pp 927−938.

(29) Ferrari, A. C.; et al. Raman Spectrum of Graphene and Graphene Layers. *Phys. Rev. Lett.* **2006**, *97*, 187401.

(30) Ferrari, A. C.; Robertson, J. Interpretation of Raman Spectra of Disordered and Amorphous Carbon. *Phys. Rev. B* **2000**, *61*, 14095–14107.

(31) Hofrichter, J.; Szafranek, B. N.; Otto, M.; Echtermeyer, T. J.; Baus, M.; Majerus, A.; Geringer, V.; Ramsteiner, M.; Kurz., H. Synthesis of Graphene on Silicon Dioxide by a Solid Carbon Source. *Nano Lett.* **2010**, *10*, 36–42.

(32) Zheng, M.; et al. A. Metal-Catalyzed Crystallization of Amorphous Carbon to Graphene. *Appl. Phys. Lett.* **2010**, *96*, 063110.

(33) Li, X.; Cai, W.; Colombo, L.; Ruoff, R. S. Evolution of Graphene Growth on Ni and Cu by Carbon Isotope Labeling. *Nano Lett.* **2009**, *9*, 4268–4272.

(34) Giovannetti, G.; Khomyakov, P. A.; Brocks, G.; Karpan, V. M.; Brink, V. D.; Kelly, P. J. Doping Graphene with Metal Contacts. *Phys. Rev. Lett.* **2008**, *101*, 026803.

(35) Lander, J. J.; Kern, H. E.; Beach, A. L. Solubility and Diffusion Coefficient of Carbon in Nickel: Reaction Rates of Nickel-Carbon Alloys with Barium Oxide. *J. Appl. Phys.* **1952**, *23*, 1305–1309.

(36) Mclellan, R. B. The Solubility of Carbon in Solid. Gold, Copper and Silver. *Scr. Metall.* **1969**, *3*, 389–391.

(37) Yamaguchi, T. Electronic Properties of Carbonized Polyacrylonitrile Fibers. *Carbon* **1964**, *2*, 95–96.